Ultrafast fluorescence studies of excited-state dynamics of a few organic chromophores in solution

van Veldhoven, E.

Publication date
2003

Citation for published version (APA):
van Veldhoven, E. (2003). *Ultrafast fluorescence studies of excited-state dynamics of a few organic chromophores in solution*. [, Universiteit van Amsterdam].

Chapter 3

Subpicosecond Fluorescence Dynamics of Organic Light-Emitting Diode Tris(8-hydroxyquinoloine) Metal Complexes

Abstract

For a few complexes belonging to a new class of organic light-emitting diodes (OLED), namely Al(III)- and Ga(III)- tris-8-hydroxyquinoline (Alq_3 and Gaq_3), femtosecond fluorescence upconversion measurements are reported. The fluorescence decays contain picosecond components when the complexes are dissolved in liquid solution. The fast components are not found in the time-resolved fluorescence of the complexes doped in an inert host crystal. The results in liquid solution are characteristic of a dynamic Stokes shift due to the solvation in a ligand-localized excited state. Furthermore, from the temporal behavior of the total fluorescence intensity it is concluded that, concomitant with solvation, adiabatic electron transfer takes place.

3.1 Introduction

The aluminum (III) 8–hydroxyquinoline complex (Alq_3) is one of the most common compounds used in the newest class of organic light emitting diodes (OLED's) [1 – 5]. To better understand the mechanisms and the dynamics of charge injection, charge transport, and charge recombination, several studies concerning the excited states of Alq_3 have been undertaken [6 – 12] From electroabsorption and -luminescence, as well as computational studies it was concluded that the lowest electronic states derive from $\pi \rightarrow \pi^*$ excitations. The lowest $^1\pi\pi^*$ state is localized at one of the quinolinolate ligands with electronic charge being partially transferred from the phenoxide to the pyridyl side of the ligand [1, 11 - 13]. Upon photoexcitation Alq_3 gives rise to a fluorescence, both in solution and in the solid state. The fluorescent state decays monoexponentially, with a typical lifetime of 10 ns [1, 6, 13] Since in organic light emitting diodes the electroluminescence is often assigned to the radiative decay of the photoemissive state [14] it is important to investigate also in this regard the photodynamics of Alq_3 in the excited state in more detail. In this Letter, we report preliminary results of our high-time resolution studies of the fluorescence of aluminum (III) 8-hydroxyquinoline, and its gallium analogue. Utilizing the fluorescence upconversion technique, we study the excited-state dynamics of Alq_3, Gaq_3 and the uncoordinated 8-hydroxyquinoline ligand, with 150 fs time resolution. The fluorescence upconversion method has in recent years been of significant importance in ultrafast studies of a wide variety of molecular systems, mainly fluorescent organic probe molecules [15 – 19]. A major advantage of the technique is that one selectively monitors the temporal behavior of the emissive state population, without interference from the ground state dynamics. Here we show the first application of this technique to an organometallic compound. We focus on the excited states of the molecular Al- and Ga complexes, both in liquid solution and host crystal, before embarking on a study of the dynamics of the same complexes in the LED layer itself.

3.2 Experimental

Alq_3 and 8-hydroxyquinoline were purchased from Aldrich and used without further purification. The fluorescence of Alq_3 was measured for the probe molecule both in liquid solution and doped (1:1000) in a host crystal of Al(acetylacetonate)$_3$ (Aldrich). The latter was grown from a solution of DMF. The Gaq_3 was synthesized as described in the literature [20]. A solution of 2.15 mmol 8-hydroxyquinoline in 100 ml 1 M acetic acid was added dropwise to a solution of 0.60 mmol $GaCl_3$ (Aldrich) and 64.87 mmol ammonium acetate (Aldrich) in 50 ml bidistilled water. The yellow crop was washed with bidistilled water, recrystallized from methanol. Steady-state absorption spectra were recorded by means of a conventional spectrophotometer (Shimadzu, UV-240). The steady-state fluorescence spectra were measured using the emission spectrometer described before [17]. The emission spectra were corrected for the wavelength-dependent sensitivity of the monochromator-photomultiplier detection system.

Femtosecond and picosecond fluorescence transients were measured by means of two experimental set-ups. Femtosecond laser excitation was accomplished using a diode-pumped cw Nd:YVO_4 laser (Spectra Physics, Millennia X) which pumped a Ti:sapphire laser (Spectra Physics, Tsunami) operating at 800 nm and which delivered 60 fs pulses at a repetition rate of 82 MHz. The laser pulses were first amplified in a regenerative amplifier laser system (Quantronix) to about 400 mW at 1 kHz, and then splitted into two beams. One of the beams was led into an OPA laser system (Light

Conversion Ltd.). The sample was moving back and forth perpendicular to the excitation laser beam from the OPA laser to avoid heating of the sample. The ensuing transient fluorescence was time-resolved detected applying the fluorescence up-conversion detection technique [16, 21]. In the latter experiments, an attenuated part of the fundamental beam (800 nm), was led through a delay line and focussed together with the pump-pulse induced fluorescence onto a 1 mm thick BBO crystal (type I phase matching condition). The up-conversion signal (at the sum frequency of the fluorescence and the fundamental of the femto-second laser) was filtered out by an UG 11 filter, and then focussed on the entrance slit of a Zeiss M 20 monochromator and photodetected using a photomultiplier (EMI, 9863 QB/350) connected to a lock-in amplifier system (Stanford Research Systems, SR 830). To avoid detection of kinetics due to reorientational motions of the probed molecules in liquid solution, the polarization of the excitation beam was at magic angle of 54^0 44' with respect to the vertically polarized gating beam. From the measured cross-correlation function of the excitation and gating pulses at 400 nm and 800 nm, the instrumental time response was estimated to be approximately 150 fs (FWHM).

Fluorescence transient measurements with picosecond time resolution were conducted using the time-correlated single-photon-counting technique [17]. Briefly, a mode-locked Ar^+ ion laser (Coherent, Innova 200-15) synchronously pumped a dye laser (Coherent, 702-3) with a cavity dumper (Coherent, 7200). The cavity-dumped dye laser generated laser pulses of about 7 ps (FWHM autocorrelation trace) and 25 nJ at 3.7 MHz. These pulses were then frequency doubled in a 6 mm BBO crystal, and used to photoexcite the sample. The fluorescence transients were detected applying the time-correlated single-photon-counting technique in reverse mode. The instrument response was about 16 ps (FWHM). All fluorescence transients were measured at magic angle.

3.3 Results

3.3.1 Alq$_3$

Steady-state absorption and emission spectra of Alq$_3$ in DMF are shown in Fig. 3.1b. The maximum of the lowest absorption band lies at 26400 cm^{-1}, while the emission band maximum is centered at 19000 cm^{-1}.

A few typical fluorescence upconversion transients of Alq$_3$ in DMF at different detection wavelengths (in the range 460 – 645 nm) for a fixed excitation ($\lambda_{exc} = 350$ nm) are shown in Fig. 3.2a.

The fluorescence decay transients were fitted to a biexponential function, convoluted with the system response. The slower of the two time constants in the biexponential function was kept fixed and equal to the lifetime of the fluorescent state. Thus the tails of the decay curves also fitted to the fitted curves of the transients obtained with the single-photon counting picosecond experiments. The different time components (τ_i) and the ratio (a_1/a_2) of the preexponential factors (a_i) for different detection wavelengths are listed in Table 3.1.

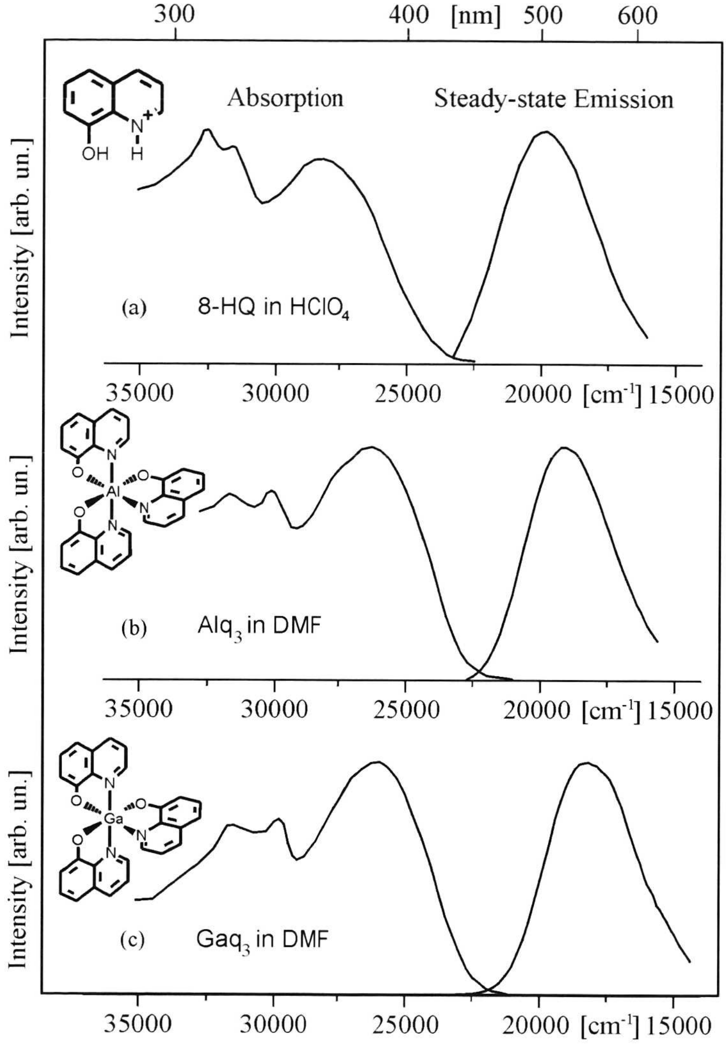

Figure 3.1: Absorption and emission spectra of a) 8-HQ in 12 M $HClO_4$ and b) Alq_3 and c) Gaq_3 in DMF

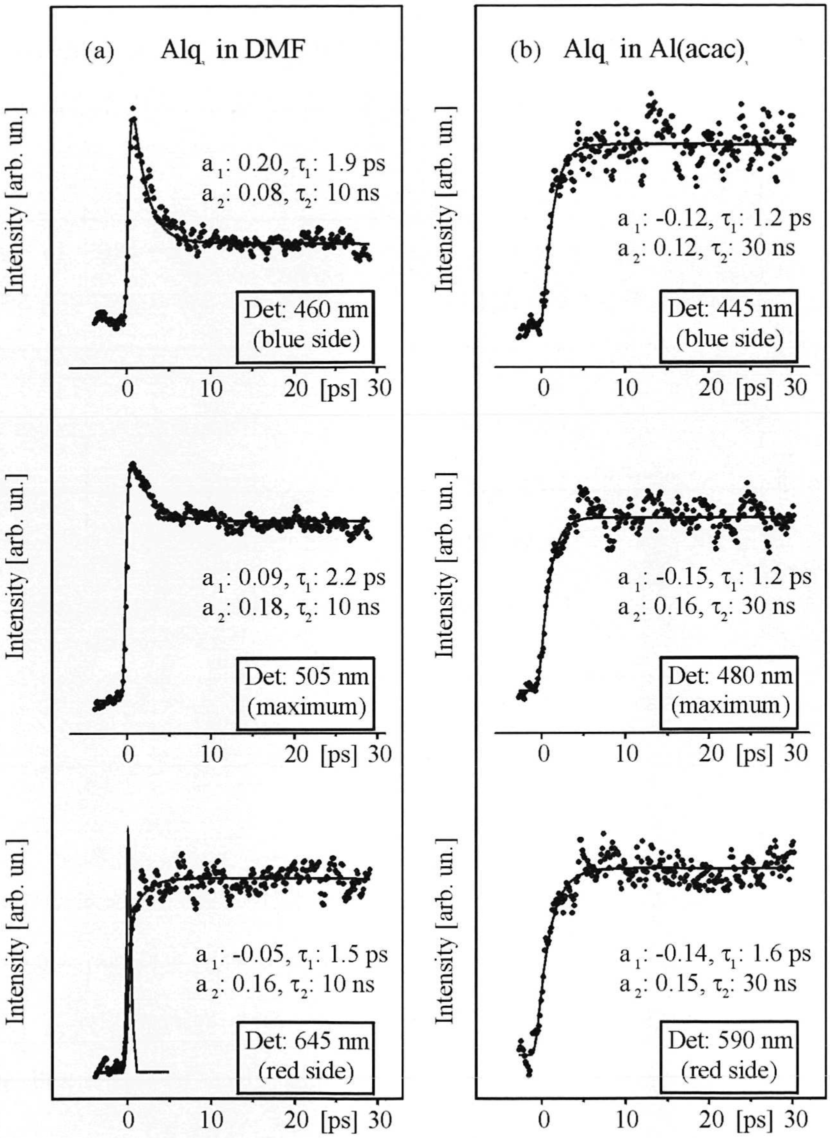

Figure 3.2: Representative fluorescence transients of Alq$_3$ a) dissolved in DMF and b) doped into Al(acac)$_3$-crystals. Drawn curves represent best fits as described in text. Respective time constants and preexponential factors are given in Table 1. The system response function is included in lowest figure of panel (a).

Table 3.1: Time components (τ_i) and preexponential factors (a_i) obtained from a biexponential fit of fluorescence decays of Alq$_3$ in DMF, measured by upconversion technique in a time window of 150 fs-33 ps, at a few representative wavelengths (λ_{exc} = 350 nm). (*) a_1 is negative.

λ (nm)	τ_1 (a_1/a_2)	τ_2
460	1.9 ps (2.44)	10 ns
480	1.9 ps (1.01)	10 ns
505	2.2 ps (0.50)	10 ns
570	0.6 ps (-0.45)*	10 ns
600	1.0 ps (-0.38)*	10 ns
645	1.5 ps (-0.31)*	10 ns

Clearly, the decay behavior upon detection at the blue side of the emission is characterized by one fast and one slow decay component, while detection at the red side exhibits a fast rising component followed by a slow decay, respectively.

Following the spectral reconstruction method given by Maroncelli and Fleming [22], time-resolved emission spectra were obtained. After fitting the resulting point-to-point spectra to a log-normal lineshape function, the drawn spectra of Fig. 3.3a for Alq$_3$ in DMF, for various times, are obtained. The figure clearly illustrates that in a time window from 300 fs up to 10 ps a spectral shifting (of about 1000 cm^{-1}) to the red takes place. The shift is accompanied by spectral broading of about 400 cm^{-1}. It also appears from Fig. 3.3a that the integrated emission intensity of the reconstructed spectra decreases with time. In Fig. 3.3b we present the data points of the integrated emission intensity of the reconstructed spectra as a function of the transition frequency corresponding to the emission band maximum.

The Alq_3 fluorescence transients were also measured for the solute in solvents of different polarity. The absorption and luminescence spectra exhibit almost no shift of the band maxima in the different solvents. However, the fluorescence decay behavior of Alq_3 is affected by the surrounding solvent. This is reflected in the respective τ_i values shown in Table 3.2.

Table 3.2: Comparison of fast decay component of Alq_3 detected at 480 nm in different solvents with typical solvent relaxation times

Solvent	τ_1 [ps] of Alq	τ [ps] Solvent [22, 23]
DMSO	2.5 ± 0.2	2.3
DMF	1.9 ± 0.2	1.7
Toluene	2.1 ± 0.2	2.2
CH_2Cl_2	0.8 ± 0.2	1.0

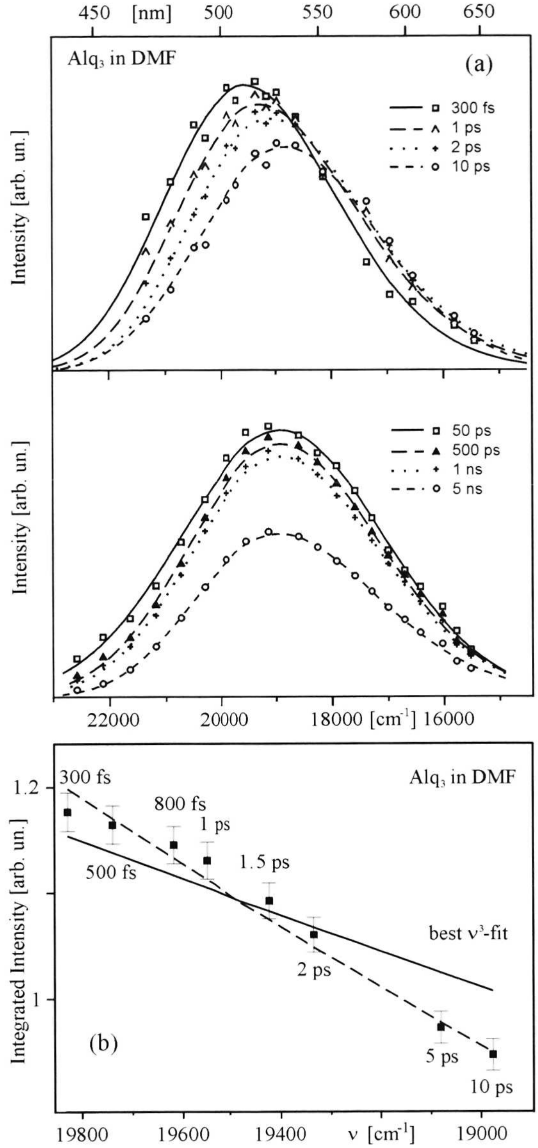

Figure 3.3: a) Reconstructed time-resolved emission spectra of Alq_3 in DMF, in the time range from 300 fs to 5 ns. b) Dependence of the integrated emission intensity of the reconstructed spectra of Alq_3 in DMF versus the transition frequency (ν/cm^{-1}). Best fit curve is of the form $p\nu^x$, with $x = 5.1$ (dashed curve). The curve with $x = 3$ is also given (dotted curve).

Alq_3 doped in the $Al(acac)_3$ host crystal showed a fluorescence spectrum similar to those of the molecule in liquid solutions. The fluorescence decay was found to be exponential with a time constant of 30 ns. In contrast to the results in liquid solution, no picosecond decay components were observed when measuring the time dependence of the fluorescence (cf Fig. 3.2b). However, a picosecond rise was found over the whole range of emission.

3.3.2 Gaq_3

Fig. 1c shows the steady-state absorption and emission spectra of Gaq_3 in DMF. The maximum of the lowest absorption band lies at 26000 cm^{-1}, while the emission band maximum is centered at 18200 cm^{-1}. As for Alq_3, also the Gaq_3 fluorescence decay transients could be fitted to a biexponential function, convoluted with the system response. The different time components (τ_i) and the preexponential factors (a_i) for different detection wavelengths are listed in Table 3.3.

Similar to the Alq_3 results, the transient behavior upon detection at the blue side of the emission is characterized by one fast and one slow decay component, while detection at the red side exhibits a fast rise followed by a slow decay. The reconstructed emission spectra of Gaq_3 in DMF for several times after the pulsed excitation are included in Fig. 3.4a. The dynamic spectral shift, as discerned from the spectra, occurs in the time window from 200 fs up to about 10 ps. Fig.3.4b shows for Gaq_3 the data points reflecting the variation of the integrated emission intensity with the transition frequency of the emission band maximum.

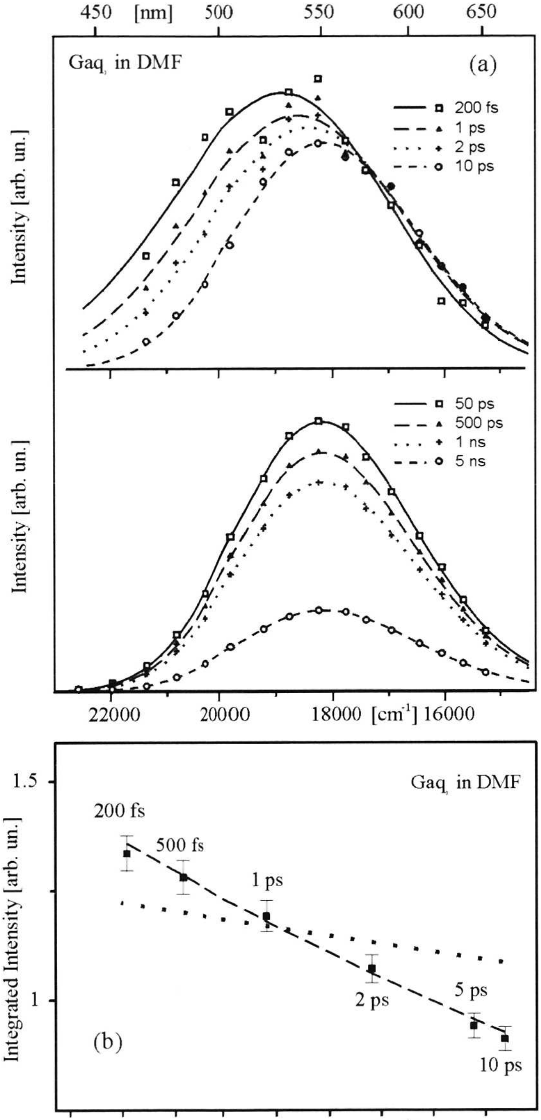

Figure 3.4. a) Reconstructed time-resolved emission spectra of Gaq$_3$ *in DMF, in the time range from 200 fs to 5 ns. b) Dependence of the integrated emission intensity of the reconstructed spectra of Gaq*$_3$ *in DMF versus the transition frequency (*ν*/cm*$^{-1}$*). Best fit curve is of the form p*ν^x*, with* $x = 9.7$ *(dashed curve). The curve with* $x = 3$ *is also given (dotted curve).*

Table 3.3: Time components (τ_i) and preexponential factors (a_i) obtained from a biexponential fit of fluorescence decays of Gaq_3 in DMF, measured by upconversion technique in a time window of 150 fs-33 ps, at a few representative wavelengths (λ_{exc} = 365 nm). (*) a_1 is negative.

λ (nm)	τ_1 (a_1/a_2)	τ_2
468	1.6 ps (3.60)	4.2 ns
480	1.9 ps (2.77)	4.2 ns
505	2.2 ps (1.21)	4.2 ns
548	2.2 ps (0.33)	4.2 ns
623	0.2 ps (-1.13)*	4.2 ns
660	1.0 ps (-0.26)*	4.2 ns

3.3.3 8-hydroxyquinoline

The respective absorption and emission band maxima for 8-hydroxyquinoline (8-HQ) in $HClO_4$ are found around 28000 cm^{-1} and 19900 cm^{-1} (Fig. 3.1a). Thus these maxima are blue shifted with respect to those for the transitions of the aluminum and gallium complexes. Fluorescence decay transients were fitted to a biexponential function, convoluted with the system response. The different time components (τ_i) and the preexponential factors (a_i) for different detection wavelengths are listed in Table 3.4.

Table 3.4: Time components (τ_i) and preexponential factors (a_i) obtained from a biexponential fit of fluorescence decays of 8-HQ in $HClO_4$, measured by upconversion technique in a time window of 150 fs-33 ps, at a few representative wavelengths (λ_{exc} = 350 nm). (*) a_1 is negative.

λ (nm)	τ_1 (a_1/a_2)	τ_2
430	1.7 ps (2.50)	1.85 ns
468	1.8 ps (0.50)	1.85 ns
480	3.4 ps (0.43)	1.85 ns
505	4.7 ps (0.18)	1.85 ns
563	1.1 ps (-0.23)*	1.85 ns
608	2.0 ps (-0.26)*	1.85 ns

Detection at the blue side of the emission spectra yields fluorescence transients characterized by a superposition of a fast and a slow decay component,

while at the red side a fast rise followed by a slow decay are detected. Time-resolved emission spectra were reconstructed from the fluorescence transients as before. The resulting spectra for 8-HQ in $HClO_4$ for several times are included in Fig. 3.5a. Dynamic spectral shifting occurs in a time window from 300 fs up to 10 ps, beyond those times no further spectral shifting was observed. The variation of the integrated emission intensity of the reconstructed spectra with the transition frequency corresponding to the emission band maximum is included in Fig. 3.5b.

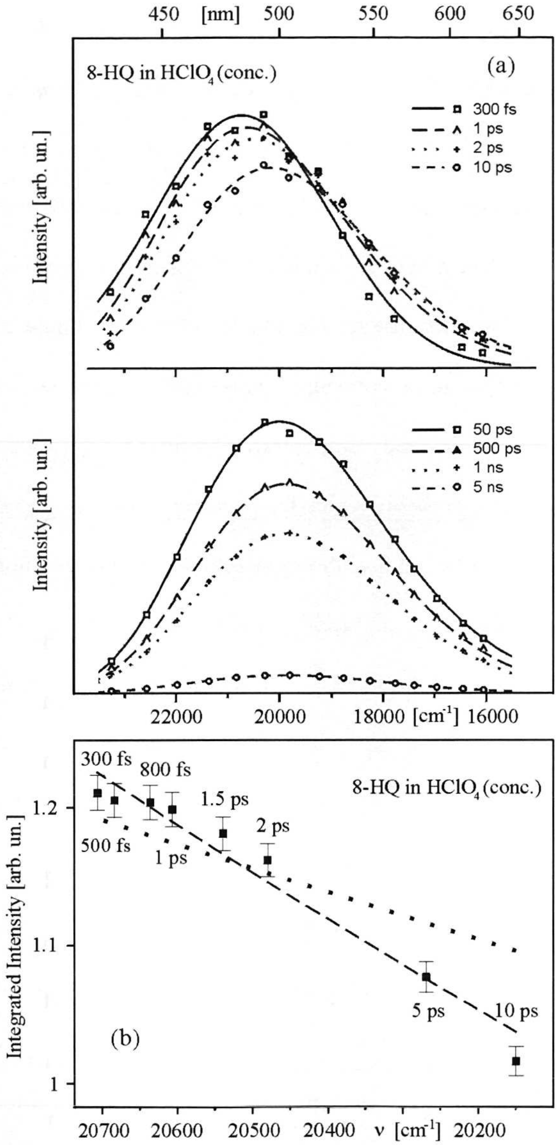

Figure 3.5: a) Reconstructed time-resolved emission spectra of 8-HQ in 12 M $HClO_4$, in the time range from 300 fs to 5 ns. b) Dependence of the integrated emission intensity of the reconstructed spectra of 8-HQ in 12 M $HClO_4$ versus the transition frequency (ν/cm^{-1}). Best fit curve is of the form $p\nu^x$, with $x = 9.7$ (dashed curve). The curve with $x = 3$ is also given (dotted curve).

3.4 Discussion

Alq_3 (aluminum (III) tris-8-hydroxyquinoline) is a tris-chelate complex, in which the metal has a distorted octahedral coordination. The two geometrical isomers of Alq_3, the "meridianal" (mer) and the "facial" (fac) isomer, are chiral and thus correspond to two different optical isomers. DFT-based calculations [12] predict that the mer isomer is lower in energy, but fac has a higher dipole moment and it is reasonable to expect that in the condensed phase both species may coexist. From ^{1}H-NMR studies [20] at elevated temperatures a ligand equilibrating process was suggested implying that probably a mer-fac exchange could take place.

As mentioned in Sec. 3.3.1, the picosecond transient components in the Alq_3 and Gaq_3 fluorescence occur in liquid solution only, and *not* in the host crystal environment. This finding suggests that the time- dependent Stokes shift following the pulsed laser excitation of Alq_3 and Gaq_3 in liquid solution, is due to the solvation process in the excited state. This is corroborated by a comparison of the short-time components in the fluorescence to the solvent relaxation times of the respective solvents. As is clear from Table 3.2, the picosecond time constants for Alq_3 and Gaq_3 nicely agree with known solvent relaxation times, as expected in the case of a dynamic Stokes shift in the continuum limit [15, 23]. It should be added that the apparent rise component in the transients obtained for the dopants in the crystal (with a typical time constant of about 1.4 ps, cf Fig. 3.2b) is due to the broadening of the response function, from 150 fs to about 1.4 ps, caused by the thickness of the crystal (2 mm).

It is of interest to note that the possibility to incorporate Alq_3 and Gaq_3 in a host crystal allows for a direct comparison of the excited-state dynamics in the liquid and the solid phase. Although this comparison is, of course, of great relevance to separate rapid decay dynamics caused by intramolecular dynamics (e.g., IVR) and intermolecular dynamics (solvation), to our knowledge, in the many studies of solvation kinetics [15, 23, 24] such an explicit comparison, has not yet been reported.

In Figs. 3.3b, 3.4b, and 3.5b, the squares are representative of the integrated intensity of the emission band as evaluated for the reconstructed band spectra at the various delay times as a function of the frequency of the emission band maximum. For illustrative purposes the figures include a best fit of the data points to a function of the form, $p\nu^x$, where it is noted that *a priori*, no physical meaning should be given to this function. The best fit values for x are 5.1 (Fig. 3.3b), 9.7 (Fig.3.4b), and 5.9 (Fig. 3.5b). Comparison of the curves with the experimental data points shows that the integrated fluorescence intensity deviates appreciably from a ν^3 dependence. (The latter, of course, is expected in case the Einstein relation for spontaneous emission holds [25]). Thus, on the one hand the excited state dynamics may be viewed as usual, i.e., it results from a relaxation of the system in a single excited electronic state (and thus give rise to the characteristic solvation times, see previous paragraph), on the other hand, the disparity with the ν^3 dependence indicates that, as the solvation takes place, the radiative character of the emissive state is changed. Both observations can be reconciled when it is assumed that solvation involves relaxation along an adiabatic potential energy surface characteristic of an emissive electronic state for which the wavefunction shows a gradual change-over as solvation progresses.

For Alq_3 it has been proposed that the fluorescent excited state is a $^1\pi\pi^*$ ligand localized state [1, 11, 12]. This is further supported by a comparison of the photokinetics for Alq_3 and 8-HQ. To compare the uncoordinated 8-HQ to the situation of coordinated ligand in the aluminum and gallium complexes, we investigated the 8-HQ in concentrated $HClO_4$ ($c \approx 12$ M), where the N-protonated species 8-HHQ^+ [26, 27] is formed. Therein, the positively charged pyridyl moiety acts as a strong acceptor, and thus enhances effectively donor-acceptor transitions from the phenoxide donor. As mentioned in Sec. 3.3, both molecular systems in liquid solution, the uncoordinated ligand as well as the coordination compounds Alq_3 and Gaq_3, show a very similar time-dependence of the fluorescence, containing rise and picosecond decay components (depending on the detection wavelength) and a similar lifetime of the relaxed excited state. The large similarity in the kinetics of the fluorescence of the 8-HHQ^+ species on the one hand and the Alq_3 and Gaq_3 complexes on the other hand, is additional evidence that in the Alq_3 and Gaq_3 complexes the emissive state is localized on an individual ligand.

The temporal behavior of the fluorescence integrated intensity (*vide supra*) indicates that the fluorescent molecules are not directly prepared in the final $^1\pi\pi^*$ state, the latter being assumed to be of charge-transfer type (electronic charge being transferred from the pyridyl ring to the quinoline group [1, 11, 12]). On the contrary, the formation of the charge-transfer state seems to follow the solvation process and thus will be completed only after approximately 10 ps. We conjecture that the electronic wavefunction is a superposition (mixture) of several zero-order wavefunctions in which the coefficients of the latter are solvation-coordinate dependent. As a result, during the solvation the electronic wavefunction is modified. Molecular orbital calculations carried out for the isolated Alq_3 suggest that the lowest singlet states S_1, S_2 and S_3 are localized on an individual quinolinolate ligand and to within ≈ 0.1 eV (≈ 800 cm^{-1}) separated from each other [11]. Solvent-induced mixing may therefore adiabatically accompany the solvation process and concomitantly affect the radiative character of the excited state in time. Note that it is implicit to this conjecture that the charge separation process within the quinolinolate ligand is also complete in about 10 ps after photoexciting the molecules. Finally, we remark that since the temporal behavior of the fluorescence observed for the Al- and Ga complexes is fully accounted for by solvation, additional dynamics as for instance due to ligand exchange phenomena [20] remain unobserved on the picosecond time scale.

In summary, a dynamic Stokes shift after pulsed laser excitation of Alq_3 and Gaq_3 in liquid solution has been concluded from fluorescence upconversion experiments with 150 fs time resolution. The dynamic spectral shift is controlled by solvation dynamics on a picosecond time scale. It was verified that the fast dynamic Stokes shift is absent in the fluorescence kinetics of the Alq_3-complex doped in a crystalline $Al(acac)_3$-matrix. From a comparison of the fluorescence kinetics of the uncoordinated ligand with that of the metal complexes, additional evidence that in the metal complex the emissive charge transfer state is localized on an individual quinolinolate ligand is obtained.

References

[1] C.W. Tang, S.A. VanSlyke, C.H. Chen, J. Appl. Phys. 65 (1989) 3610.

[2] P.E. Burrows, L.S. Sapochak, D.M. McCarty, S.R. Forrest, M.E. Thompson, Appl. Phys. Lett. 64 (1994) 2718.

[3] J. Kido, M. Kimura, K. Nagai, Science 267 (1995) 1332.

[4] P.E. Burrows, Z. Shen, V. Bulovic, D.M. McCarty, S.R. Forrest, J.A. Cronin, M.E. Thompson, J. Appl. Phys. 79 (1996) 7991.

[5] J.R. Sheats, H. Antoniadis, M. Hueschen, W. Leonard, J. Miller, R. Moon, D. Roitman, A. Stocking, Science 273 (1996) 884.

[6] R. Ballardini, G. Varani, M.T. Indelli, F. Scandola, Inorg. Chem. 25 (1986) 3858.

[7] A.D. Walser, I. Sokolik, R. Priestley, R. Dorsinville, Synthetic Metals 84 (1997) 877.

[8] R. Priestley, I. Sokolik, A.D. Walser, C.W. Tang, R. Dorsinville, Synthetic Metals 84 (1997) 915.

[9] I. Sokolik, A.D. Walser, R. Priestley, C.W. Tang, R. Dorsinville, Synthetic Metals 84 (1997) 921.

[10] L.-J. Lin, S.A. Jenekhe, R.H. Young, P.M. Borsenberger, Appl. Phys. Lett. 70 (1997) 2052.

[11] W. Stampor, J. Kalinowski, G. Marconi, P. Di Marco, V. Fattori, G. Giro, Chem. Phys. Lett. 283 (1998) 373.

[12] A. Curioni, M. Boero, W. Andreoni, Chem. Phys. Lett. 294 (1998) 263.

[13] F.E. Lytle, D.R. Storey, M.E. Juricich, Spectrochim. Acta 29A (1973) 1357.

[14] J.H. Burroughes, D.D.C. Bradley, A.R. Brown, R.N. Marks, K. Mackay, R.H. Friend, P.L. Burns, A.B. Holmes, Nature 347 (1990) 539.

[15] M.L. Horng, J.A. Gardecki, A. Papazyan, M. Maroncelli, J. Phys. Chem. 99 (1995) 17311.

[16] M.A. Kahlow, W. Jarzeba, T.P. Dubrull, P.F. Barbara, Rev. Sci. Instrum. 59 (1988) 1098.

[17] E.R. Middelhoek, P. van der Meulen, J.W. Verhoeven, M. Glasbeek, Chem. Phys. 198 (1995) 573.

[18] P. Changenet, H. Zhang, M.J. van der Meer, K.J. Hellingwerf, M. Glasbeek, Chem. Phys. Lett. 282 (1998) 276.

[19] P. Prosposito, D. Marks, H. Zhang, M. Glasbeek, J. Phys. Chem. A 102 (1998) 8894.

[20] H. Schmidbaur, J. Lettenbauer, D.L. Wilkinson, G. Müller, O. Kumberger, Z. Naturforsch. 46b (1991) 901.

[21] H. Zhang, A.M. Jonkman, P. van der Meulen, M. Glasbeek, Chem. Phys. Lett. 224 (1994) 551.

[22] M. Maroncelli, G.R. Fleming, J. Chem. Phys. 86 (1987) 6221.

[23] L. Reynolds, J.A. Gardecki, S.J.V. Frankland, M.L. Horng, M. Maroncelli, J. Phys. Chem. 100 (1996) 10337.

[24] A.E. Johnson, K. Tominaga, G. C. Walker, W. Jarzeba, P.F. Barbara, Pure Appl. Chem. 65 (1993) 1677.

[25] T. Förster, Fluoreszenz organischer Verbindungen (Vandenhoeck and Ruppert, Göttingen, (1951).

[26] E. Bardez, A. Chartelain, B. Larrey, B. Valeur, J. Phys. Chem. 98 (1994) 2357.

[27] E. Bardez, I. Devol, B. Larrey, B. Valeur, J. Phys. Chem. B 101 (1997) 7786.